Tomographic investigation of the influence of wall effects on the breakthrough in a highly loaded packed bed adsorber

Karijm Salem[1], Witold Kwapinski[2], Evangelos Tsotsas[2], Dieter Mewes[1]

[1] Institute of Process Engineering, University of Hannover, Callinstrasse 36, D-30167 Hannover, Germany

[2] Thermal Process Engineering, University of Magdeburg, Universitätsplatz 2, D-39106 Magdeburg, Germany

Abstract

An optical tomographic measurement technique is developed that enables non-intrusive concentration field measurements at the outlet of a packed bed adsorber. The measurement technique stands out with a high time and spatial resolution, a maximum measurement frequency of 20Hz and a spatial resolution of 0.02% related to the measurement cross-section. It is applied on the investigation of wall effects on adsorbtion occurring in a packed bed with a low ratio between tube and particle diameter of $D/d_p=11$. The measured concentration fields point up that for the design of such packed bed adsorbers, the breakthrough must be regarded not only in respect to time, but also in respect to the radial coordinate.

1. Introduction

The separation of gas mixtures in the industrial production is mostly performed using rectification and absorption. These techniques are integrated in continuous production processes allowing a high throughput. In times of strict pollution control especially separation of low concentrations must be accounted for. For this purpose both techniques are not profitable. It is rather the adsorption technique that convinces with efficient separation of trace levels of gas components. This makes the adsorption as well most suitable for dehumidifying process gases necessary for example during the semiconductor fabrication process or dehumidifying natural gas for liquefaction using molecular sieves.

The adsorption is usually conducted in packed bed columns as batch process. As thermal separation process it is accompanied by a strong heat release. This sorption heat affects the process adversely by reducing the adsorbent capacity significantly. Therefore low-diameter columns are applied which can be actively cooled by the column wall. In such columns with a low tube to particle diameter ratio the velocity profile shows a maximum near the wall due to the locally higher porositiy. The influence of this channeling on the adsorption process must not be neglected. Münstermann (1984) and Lingg (1995) have already analyzed channeling effects. Because both authors used measurement probes in the column to drain off the gas the interference with the flow field cannot be excluded. Münstermann positioned the probes at a fixed position at the column outlet covering a quarter of the complete cross-section. The author reported mean concentrations for the wall region and the centre of the bed. Lingg measured the radial and axial concentration profile

selectively and one after another by single measurement probes. Especially for the non-stationary flow in the adsorption column this measurement techniques is not adequate.

The lack of high temporal and spatial concentration measurement data for adsorption columns demands a superior measurements technique. The only way to acquire these data non-intrusively is by means of optical methods. Fluid concentrations measurements using the laser absorption spectroscopy yield only information about the concentration along a line of sight. But these mean concentrations stand out with a high resolution and accuracy as known from the quantitative spectroscopy (Talsky, 1994).

First Kauranen et al. (1994) combined the laser absorption spectroscopy and tomography to extract the missing local information by the tomographic reconstruction technique. The authors reported the measurement of mean O_2 concentrations over time in a stationary gas flow using a single laser beam and traversing the measurement object. Hindle et al. (2001) extended this technique for acquiring concentration profiles in a non-stationary hydrocarbon gas flow using altogether 32 parallel beams from 4 directions. Although the author reported a high temporal resolution of 3000 frames per seconds the spatial resolution is limited due to the low number of beams in the measurement cross-section.

To provide non-intrusive high temporal and spatial resolution concentration measurements of moisture in an adsorption column (50mm diameter) a new optical tomography device is developed.

2. Optical Setup

The optical setup for the developed measurement device is shown in figure 1. The complete setup is encased in a box to keep the moisture constant along the rays. The light source is a diode laser with a wavelength at 1396.5nm. In this wavelength region several absorption bands of water vapor are located.

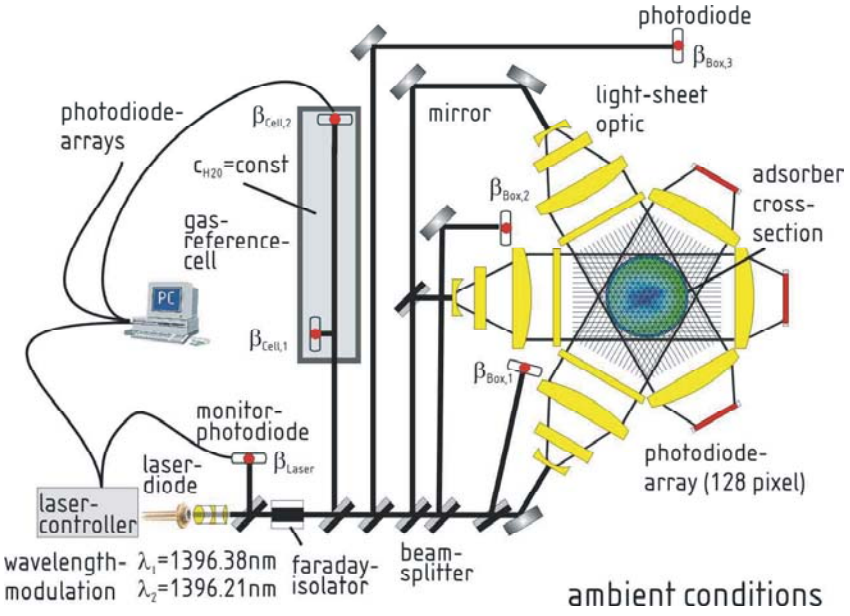

Figure 1. Optical set-up (schematically)

The collimated laser beam is divided into three beams of equal intensity using beam-splitters. Then each beam is expanded to a light-sheet using cylindrical lenses. After propagating the adsorber cross-section the intensity profiles of the light sheets are recorded with detector arrays (InGaAs) simultaneously. The detector arrays provide a resolution of 128 pixels and allow a maximum measurement frequency of 300Hz. The intensity measured by each detector array pixel contains the information for calculating the mean concentration along the corresponding ray path. The relation between intensity I and concentration C is generally described by the Lambert-Beers law

$$C = -\frac{1}{l \cdot \varepsilon} \ln\left(\frac{I}{I_0}\right), \tag{1}$$

where l is the path length, ε the extinction coefficient of the absorbing species and I_0 the reference intensity for a concentration of C=0 mol/l without absorption.

In spite of using high loads during adsorption result in a fast breakthrough it needs several hours until the total equilibrium of the bed is achieved. This requires next to a high temporal resolution for the beginning of adsorption a strong long-term stability of the measurement system.

3. Stabilizing the measurement device for long-term measurements

The advantages using a DFB laser diode are a small line-width and tunability in the wavelength range of 5 nm. But due to the strong temperature dependence of its output intensity and wavelength, a precise temperature control is necessary. This temperature control is realized using a thermoelectric cooler and thermistor that are connected to the laser diode. Nevertheless, an intensity drift during long-term measurements is observed, which affects the laser wavelength as well. Additionally the collimated laser beam profile is changing. This phenomenon can be explained by spatial shifts of the waver material in the laser diode and of the optics by vibrations and thermal effects. The instabilities decrease with laser running time, but do not disappear completely.

Regarding the Lambert-Beer's law (eq.(1)) a reference measurement at C = 0 mol/l of the laser intensity profile before each concentration measurement becomes necessary. To gather the missing information without interrupting and disturbing the adsorption process a second wavelength is introduced. Thus wavelength λ_1 is modulated by the laser current to a wavelength λ_2 with weaker absorption by water vapor using a square pulse. For both wavelengths the transmission intensity is measured. Then the integrated concentration along a path length l can be expressed by

$$\int \mathrm{C}\,\mathrm{dl} = -\frac{1}{\left(\varepsilon_{\lambda 1} - \varepsilon_{\lambda 2}\right)} \ln\left(\frac{\mathrm{I}_{\lambda 1,0}}{\mathrm{I}_{\lambda 2,0}} \cdot \frac{\mathrm{I}_{\lambda 2}}{\mathrm{I}_{\lambda 1}}\right), \tag{2}$$

where the intensities $\mathrm{I}_{\lambda 1}$ and $\mathrm{I}_{\lambda 2}$ are the measurement values at both wavelengths. The reference intensities $\mathrm{I}_{\lambda 1,0}$ and $\mathrm{I}_{\lambda 2,0}$ the extinction coefficients $\varepsilon_{\lambda 1}$ and $\varepsilon_{\lambda 2}$, and the path length l are determined by calibration measurements. In terms of laser profile instabilities by spatial

shifts in the laser diode or of the optics the measurement device is self-calibrating using equation (2).

The observed laser wavelength drift affects the transmission intensities for both wavelengths differently. Because the optics is encased in a box with a constant humidity, laser light is propagating through the humid air and absorbed depending on the wavelength. With a path-length l_{Box} up to 30 times longer in the box than the maximum path-length l inside the measurement cross-section, small wavelength drifts have a strong effect on the measurement accuracy. To compensate this, four photo-diodes are installed. The intensities directly behind the laser and along the three splitted beams through the box are acquired during the measurement (Fig. 1). Using altogether 3 photodiodes for correction also maldistribution of humidity in the box is accounted for. From these data the correction factor γ_{Box} is calculated:

$$\gamma_{Box} = \frac{\theta_{Laser}}{\theta_{Laser,t=0}} \cdot \left(\frac{\theta_{Box} \cdot \theta_{Laser,t=0}}{\theta_{Box,t=0} \cdot \theta_{Laser}} \right)^{\left(\frac{l_{Box}}{l}\right)}, \tag{3}$$

$$\theta = \frac{I_{\lambda 1}}{I_{\lambda 2}} \tag{4}$$

where θ is the intensity ratio for both wavelengths. The index “t=0” indicates the ratio at the beginning of the measurement. The index “Laser” represents the intensity ratio directly behind the laser, and the index “Box” the intensity ratio for the corresponding photo-diode in the box. l_{Box} is the pathway in the box excluding the measurement cross-section. The correction factor γ_{Box} is inserted into eq.(2), leading to the relationship:

$$\int C dl = -\frac{1}{(\varepsilon_{\lambda 1} - \varepsilon_{\lambda 2})} \ln\left(\frac{I_{\lambda 1,0}(t_0)}{I_{\lambda 2,0}(t_0)} \cdot \frac{I_{\lambda 2}(t)}{I_{\lambda 1}(t)} \cdot \gamma_{Box} \right). \tag{5}$$

Changes of wavelength do affect the concentration measurements as well. Therefore changes of the extinction coefficients have to be considered. The change of the extinction coefficient with time is acquired using a gas reference cell as shown in Fig. 1. The cell is filled with constant water vapor concentration and the transmission intensity is measured by two photodiodes. Calculating the intensity ratios $\theta_{Cell,1}$ and $\theta_{Cell,2}$ for both photodiodes the wavelength correction factor γ_{ε} is determined to

$$\gamma_{\varepsilon} = \frac{\ln\left(\frac{\theta_{Cell,2,t=0} \cdot \kappa}{\theta_{Cell,1,t=0}} \right)}{\ln\left(\frac{\theta_{Cell,2} \cdot \kappa}{\theta_{Cell,1}} \right)}, \tag{6}$$

with factor

$$\kappa = \frac{\theta_{Cell,1}}{\theta_{Cell,2}} \tag{7}$$

determined by a measurement at reference conditions with C = 0 mol/l.

Finally, eq.(8) contains the calculation of the integrated concentration along a path length l including the correction for the laser profile, the intensity, the wavelength and the box concentration changes:

$$\int \mathrm{Cdl} = -\frac{\gamma_{\varepsilon}}{(\varepsilon_{\lambda 1} - \varepsilon_{\lambda 2})} \ln\left(\frac{I_{\lambda 1,0}(t_0)}{I_{\lambda 2,0}(t_0)} \cdot \frac{I_{\lambda 2}(t)}{I_{\lambda 1}(t)} \cdot \gamma_{\mathrm{Box}} \right) \tag{8}$$

Including all measures for the long-term stabilization the maximum measurement frequency is 20Hz.

4. Principle of tomographic image reocnstruction

Optical measurement techniques mostly measure line-of-sight projected intensities that integrate optical information along the beam path in the measurement field. To recover the cross-sectional field information from the projected images the tomographic image reconstruction is necessary. Depending on the symmetry of the field, the number of projections and projections angles a suitable reconstruction technique has to be chosen. The technique utilized here is the algebraic reconstruction technique (ART)(Gordon 1974). The reconstruction procedure is depicted in figure 2. From the measured intensity the integral concentration is calculated applying equation (8). Assuming 48 projections in each light sheet, altogether 144 equations for the three projection angles (120°) are obtained. These projections span a reconstruction field with 3252 triangular concentration field elements. The low number of equations in relation to the high number of unknown concentrations forms an under-determined equation system. Since the algorithm is iterative the reconstruction process is started with an estimation of local concentrations in the measurement field. For each projection integral concentration of the actual set is compared with the measured data. The difference is then partly added to the actual data set. The calculation is repeated for 10 cycles for the whole set of projection elements. Then the deviation related to the measured concentration is always less than 1%. The described reconstruction grid results in a spatial resolution of 0.02% in relation to the measurement cross-section.

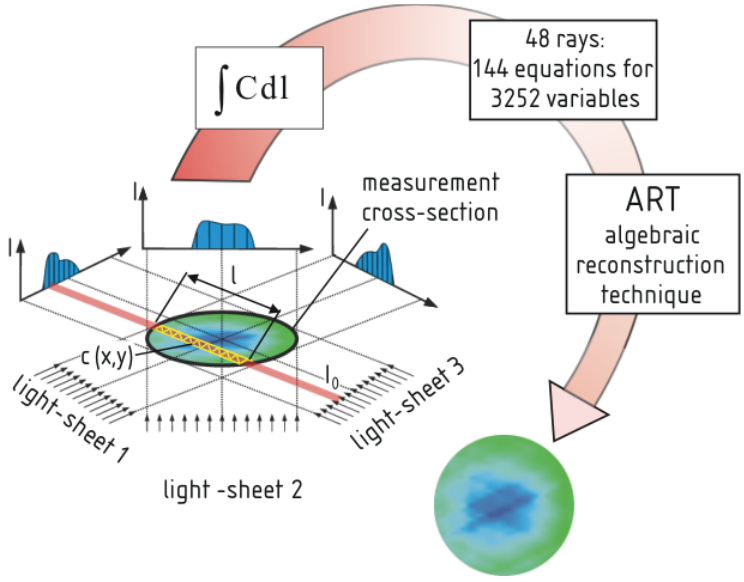

Figure 2. Principle of tomographic reconstruction.

5. Experimental setup

The developed measurement technique is applied on an adsorption column with 50mm diameter filled with molecular sieve 4Å particles (4.5mm to 5mm diameter). The bed is charged with a vapor feed containing air and water. The experimental setup is schematically shown in Fig. 3.The adsorptive water vapor is produced by atomizing water into the air stream. This mixture is evaporated in an electric heater. The resulting water vapor concentration is calculated from the air dew point, the air volume flow rate, the water mass flow rate and the temperature. The feed is conducted to the adsorption column using electrically heated pipes, which prevent condensation of water. At this position the water vapor concentration is checked using a gas infrared analyzer. The adsorption column is manufactured of stainless steel and is divided into three segments with 200 mm height each, which allows investigating different adsorber heights. Each segment is equipped with heating and cooling pipes for tempering the wall. Additionally, three heating circuits are installed at each segment to compensate temperature gradients of the heat transfer fluid flowing along the wall. The complete column is insulated using the elastomeric material Armaflex.

Thermocouples are mounted 30 mm below each segment exit to measure the radial bed temperature. To this purpose plastic ducts (material PEEK) are positioning the thermocouples at six different radial positions and insulating the sensor wires against the column wall. The outer thermocouple-duct diameter in the bed is only 3mm to minimize the influence on the flow distribution.

For the measurement of the water vapor concentration field at the adsorber exit the optical tomographic measurement device is attached. The optical access for this measurement technique is obtained by extending the column using a hollow glass cylinder (inner diameter 50 mm, height 20 mm). As reported by Schuster (1981), the maximum flow velocity at the outlet of the bed is shifted from the wall towards the centre with increasing distance from the packed bed. This, of course, affects the concentration profile. Therefore the measurement cross-section is positioned only a few millimeters above the bed. Additionally, the infrared gas analyzer measures the mean water vapor concentration. A condenser at the exit of the adsorption column prevents that condensing water drops down on the adsorbent.

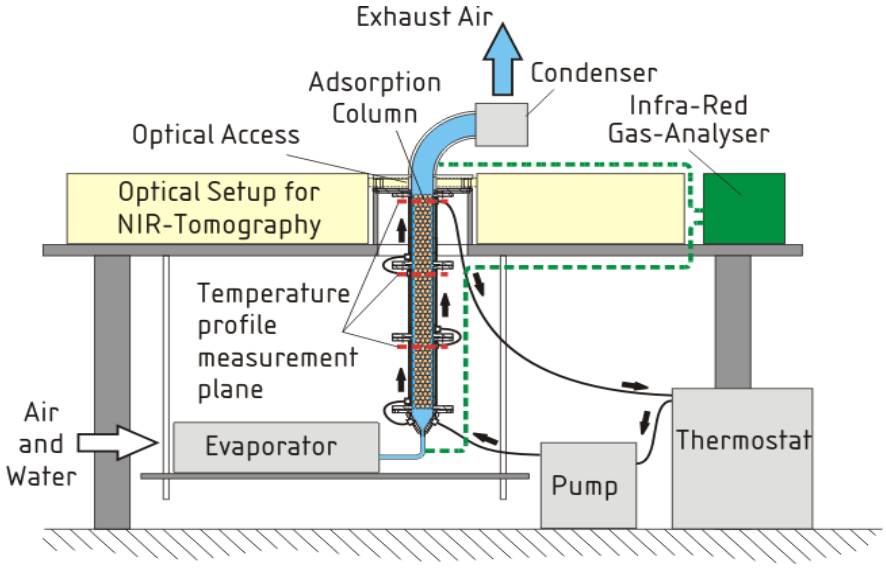

Figure 3. Overview of the experimental set-up.

6. Experimental results

Outlet concentration fields and profiles during adsorption are shown in figures 6 and 7 for one selected experiment. The radial concentration profiles are presented in figure 6 by means of transients for different annular sections. For these sections the respective average concentration has been calculated.

A single column segment with a height of 200 mm is filled with spherical molecular sieve particles narrowly sieved between 4.5 and 5 mm with an average diameter of approximately d_p = 4.75 mm. As preparation, the adsorbent particles are purged with a gas flow at 40.5 °C and a water vapor concentration of $C_0 = 5.73 \cdot 10^{-4}$ mol/l (relative humidity of φ_0 = 19.7 %) for 15 hours until the equilibrium is reached. All pipes and the column wall are temperature controlled to 40.5 °C to avoid condensation of water vapor. Then, the feed is adjusted to a constant water vapor concentration of $C_{in} = 1.4 \cdot 10^{-3}$ mol/l and the adsorption column is charged.

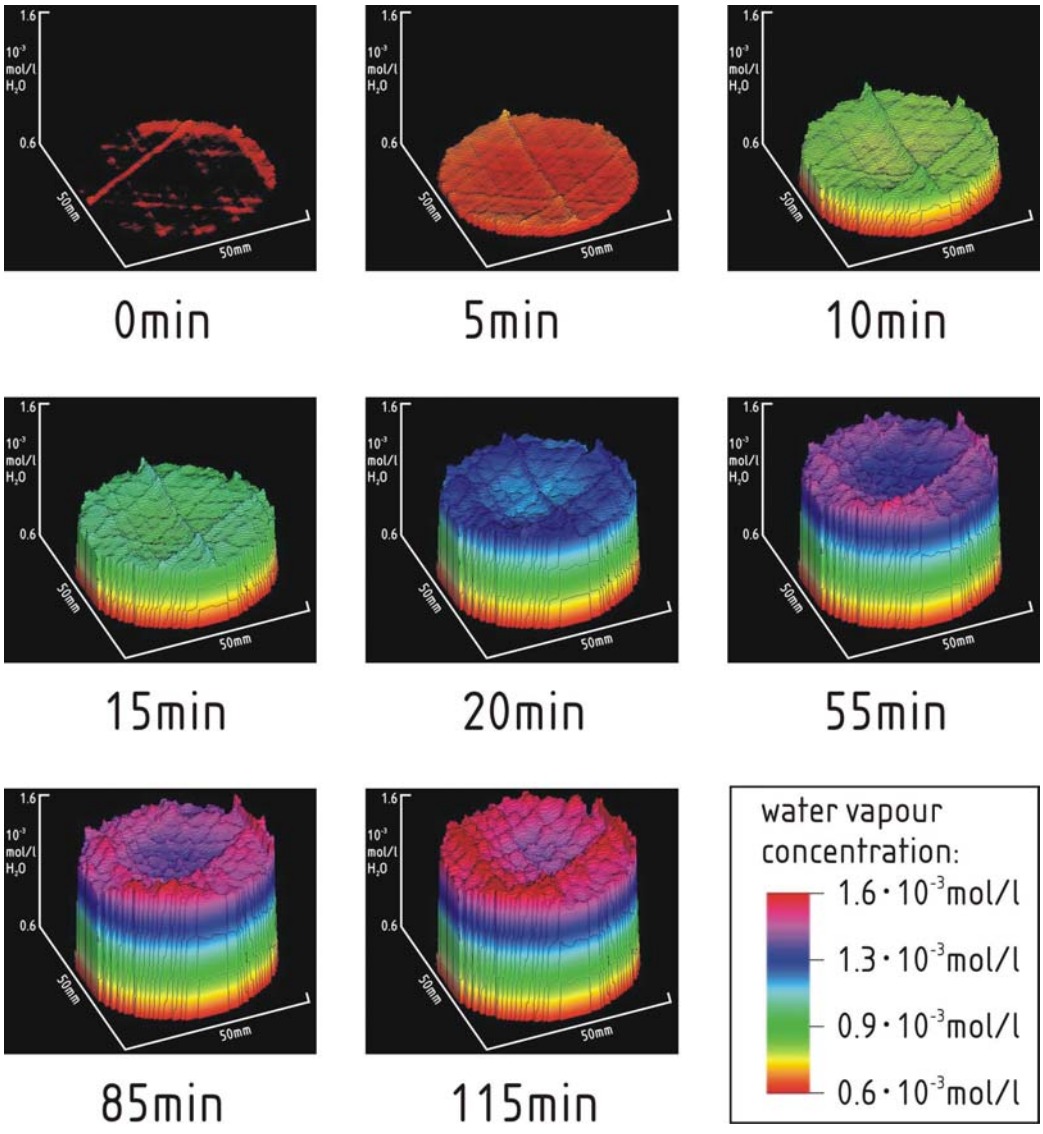

Figure 6. Concentration fields at the outer of the packed bed adsorber.

The breakthrough starts early, after approximately 5 min. The concentration at the column exit is then increasing continuously, while the concentration in the core region of the bed is at any time less than at the wall (figure 6). This behavior is the result of high velocities (channeling) and high porosities near to the column wall. As the mass transfer between feed and adsorbent proceeds and the adsorbent saturates, the feed breaks through. At the same time the temperature is increasing quickly (figure 8). After about 20 min the temperature shows a maximum near the wall and with a small time delay also in the core of the bed. As the concentration front reaches the exit of the bed, no heat is released by adsorption anymore, and the temperature decreases again.

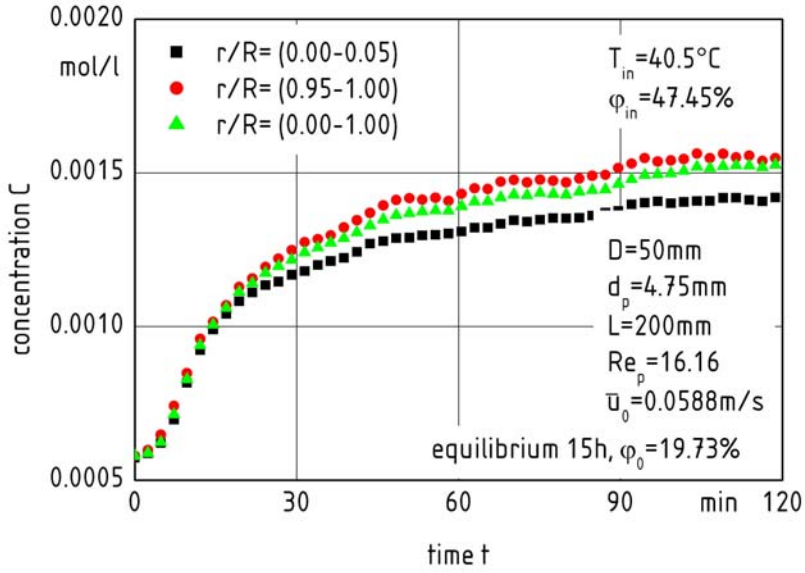

Figure 7. Concentration transients at different radial positions at the outlet of the adsorber

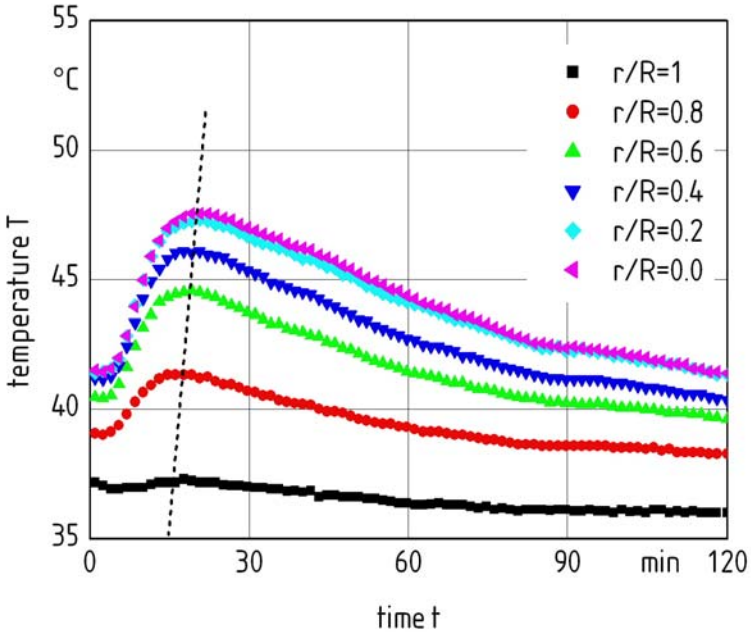

Figure 8. Temperature transients measured at different radial positions.

The concentration slope over the time is decreasing abruptly, which is more pronounced in the core than in the wall region (figure 7). This can be explained by the temperature gradient of about 10 K to the wall. The heat release by the adsorbent particles is dissipated efficiently near the wall, so that the temperature does not change too much. In the core region, however, the temperature decreases rather quickly after the hot spot has been overcome, so that the adsorption capacity of the bed increases again. With continuing adsorption the radial concentration gradient increases until the measurement is stopped after 120 min.

7. Conclusions

The investigation of concentration fields at the outlet of a packed bed adsorber needs a non-intrusive measurement technique with a high temporal and spatial resolution and a high long-term stability. Therefore an optical tomographic measurement technique is developed which achieves these high demands with a spatial resolution of 0.02% in relation to the measurement cross-section and maximum measurement frequency of 20Hz. The influence of wall effects on the breakthrough is shown by an adsorption experiment for a tube to particle diameter of 11. Due to the higher porosity and therefore higher velocity near the wall the heat and mass transfer between the feed and adsorbent is locally increased. This results in an earlier breakthrough in the wall region than in the core region of the bed.

8. Acknowledgments

The financial support of the Deutsche Forschungsgemeinschaft (DFG) is acknowledged. The authors would also like to thank Zeochem AG, CH, for the supply with molecular sieve 4Å.

9. References

Gordon, R (1974). A Tutorial on ART (Algebraic Reconstruction Technique), IEEE Transactions on Nuclear Science, 21, 78-93.

Hindle, F., Carey, S., Ozanyan, K., Winterbone, D., Clough, E., McCann, H. (2001). Measurement of gaseous hydrocarbon distribution by a Near Infra-Red absorption tomography system, *Journal of Electronic Imaging*, 10, 593-600.

Kauranen, P., Hert, M., Svanberg, S. (1994). Tomographic imaging of fluid flows by the use of two-tone frequency-modulation spectroscopy, *Optics Letters*, 19(18), 1489-1491.

Lingg, G. (1995), Die Modellierung gasdurchströmter Festbettadsorber unter Beachtung der ungleichmäßigen Strömungsverteilung und äquivalenter Einphasenmodelle, *Dissertation, Technische Universität München*

Münstermann, U., (1984). Adsorption von CO_2 aus Reingas und aus Luft am Molekularsieb-Einzelkorn und im Festbett, *Dissertation, Technische Universität München*, Germany.

Schuster, J., Vortmeyer, D. (1981), Geschwindigkeitsverteilung in gasdurchströmten, isothermen Kugelschüttungen, Chem. Ing. Tech., 53 (10), 806-807.

Talsky, G. (1994). Derivative spectrophotometry : low and higher order. Weinheim: VCH